Journal of Hydrology 401 (2011) 14–21

Contents lists available at ScienceDirect

Journal of Hydrology

journal homepage: www.elsevier.com/locate/jhydrol

Pumping test analysis using a layered cylindrical grid numerical model in a complex, heterogeneous chalk aquifer

M.M. Mansour [a,*], A.G. Hughes [a], A.E.F. Spink [b], J. Riches [c]

[a] British Geological Survey, Keyworth, Nottingham, UK
[b] The University of Birmingham, Birmingham, UK
[c] Thames Water, Reading, UK

ARTICLE INFO

Article history:
Received 2 February 2010
Received in revised form 10 January 2011
Accepted 3 February 2011
Available online 13 February 2011

This manuscript was handled by P. Baveye, Editor-in-Chief

Keywords:
Pumping test
Layered cylindrical grid model
Numerical modelling
Chalk aquifer

SUMMARY

A groundwater investigation including several pumping tests has been carried out by Thames Water Utilities Limited (TWUL) to improve the understanding of the distribution of hydraulic properties of the Chalk in the Swanscombe area of Kent in south-eastern England. The pumping test behaviour is complicated by: the fractured condition of the Chalk, simultaneous pumping from adjacent boreholes, and variable pumping rates during the test. In addition, the groundwater flow system is complicated by quarrying of the Chalk. Analytical solutions for pumping test analysis fail to represent these complex flow processes and cannot reproduce the observed time-drawdown curves. A layered cylindrical grid numerical model has been applied to the results of the Swanscombe pumping test. This model can represent the heterogeneity of the aquifer and the detailed flow processes close to the abstraction borehole such as well storage, seepage face and well losses. It also includes a numerical representation of the moving water-table using a grid that deforms to eliminate numerical instabilities. The analyses of the test results demonstrate that they are significantly influenced by fracture flow, which needs to be included to improve the simulation of the groundwater system; not withstanding this, the layered cylindrical grid numerical model reproduced many of the features in observed time-drawdown, which allowed an assessment of the hydraulic characteristics of the aquifer as well as the investigation of the impact of quarries on the test results. This has demonstrated that the numerical model is a powerful tool that can be used to analyse complex pumping tests and aid to improvement of the conceptual understanding of a groundwater system.

1. Introduction

During the later part of 2002, a multiple borehole pumping test was conducted by Thames Water Utilities Limited (TWUL) to understand the hydraulic properties of the Chalk aquifer, in the Swanscombe area of Kent in south-eastern England, and to assess abstraction sustainability (Fig. 1). Pumping tests are controlled field experiments carried out to determine the hydraulic properties of an aquifer or to validate a conceptual model of a groundwater system (BSI, 1992). Such tests yield plots of time-drawdown values which exhibit a behaviour dictated by the hydraulic characteristics of the aquifer. Under ideal conditions, this behaviour can be represented by analytical solutions to obtain the values of the hydraulic parameters of the aquifer. Typical time-drawdown plots, produced by these analytical solutions, have been described by a number of researchers, for example Neuman and Witherspoon (1971), Neuman (1979), Streltsova (1972, 1973), Gambolati (1976), and Kruseman and de Ridder (1990).

Previous studies of Chalk aquifer properties show that the transmissivity and storage coefficient vary spatially depending on the geological development of the Chalk (Allen et al., 1997). The development of fractures complicates the groundwater flow behaviour and solution processes greatly affect the characteristics of the Chalk and the flow mechanisms within it, which is often referred to as dual-porosity. It is, therefore, anticipated that the hydraulic properties of the Chalk in the Swanscombe area will be spatially variable, causing the time-drawdown curves to deviate from the typical plots. This deviation is potentially exacerbated by: the existence of large active sub-water-table quarries (Fig. 2a); simultaneous abstraction from adjacent boreholes leading to interfering cones of depression; and because of the occurrence of generator outages causing random interruption to abstraction and unplanned periods of groundwater head recovery. Consequently, the commonly used analytical solutions such as Theis (1935) solution and the Cooper and Jacob (1946) approximation for analysing

* Corresponding author. Tel.: +44 1159363509.
E-mail addresses: majm@bgs.ac.uk (M.M. Mansour), aghug@bgs.ac.uk (A.G. Hughes), a.e.f.spink@bham.ac.uk (A.E.F. Spink), Jamie.Riches@thameswater.co.uk (J. Riches).

0022-1694/$ - see front matter © 2011 British Geological Survey. Published by Elsevier B.V. All rights reserved.
doi:10.1016/j.jhydrol.2011.02.005

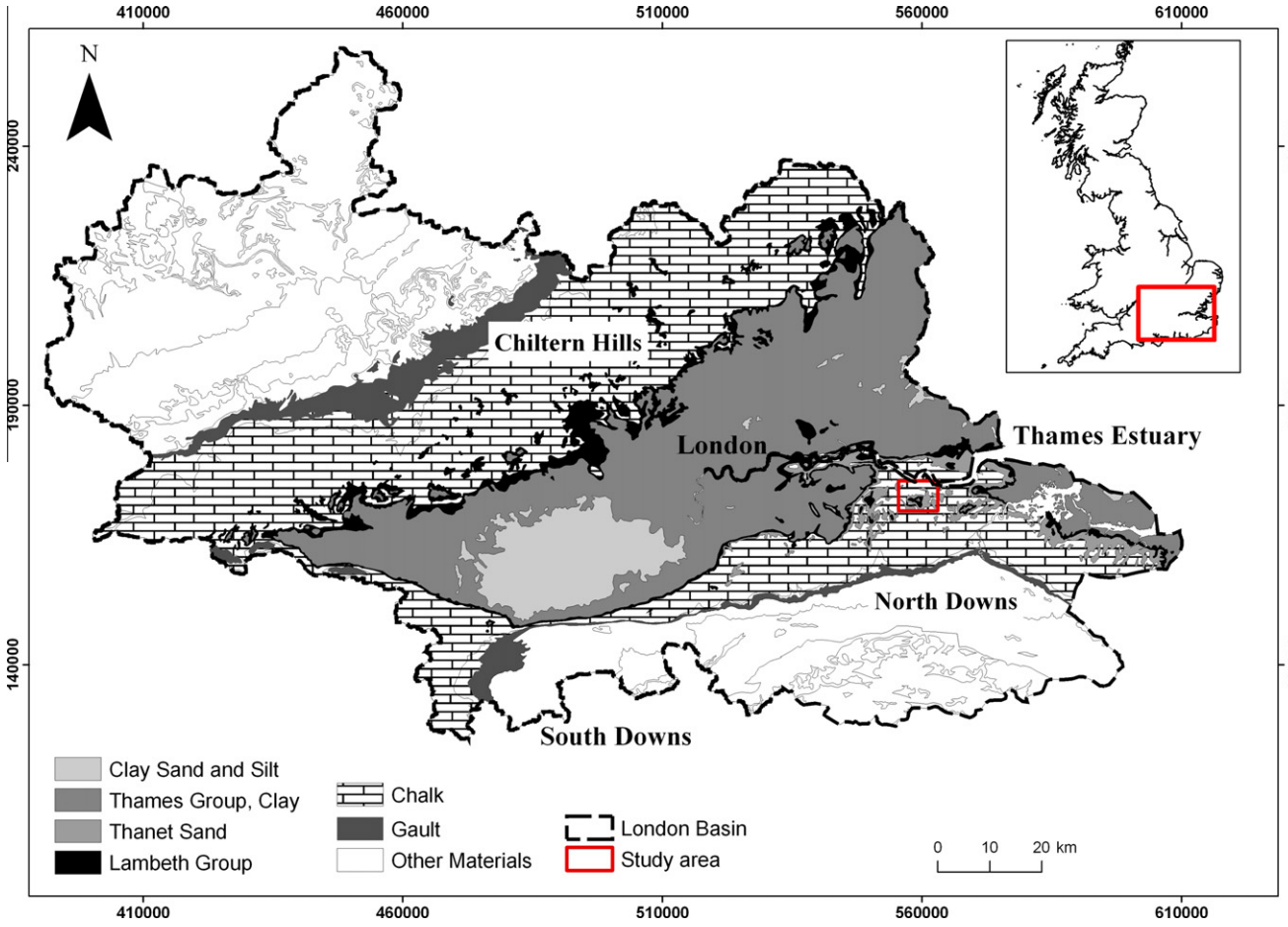

Fig. 1. Regional setting of the Swanscombe area.

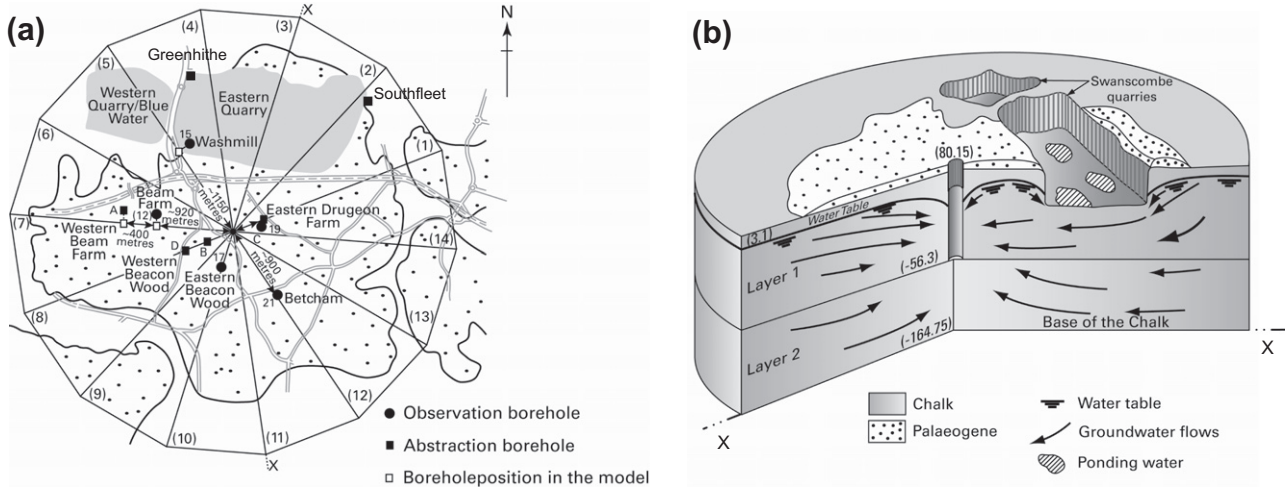

Fig. 2. Conceptual model and numerical model setting at site C.

pumping tests in confined aquifers, the Hantush–Jacob (1955) solution for leaky aquifers, Boulton's (1954) model, Dagan's (1967) solution and Neuman's (1972) equations for tests in unconfined aquifers cannot be applied effectively to the Swanscombe pumping test. Other analytical solutions such as the analytical solution for partially penetrating wells in unconfined aquifers (Neuman, 1974) or (Moench, 1993, 1994), the analytical solution that accounts for pumping from large diameter wells in unconfined aquifers (Moench, 1997), the solution for unsteady flows in single-porosity or double-porosity confined aquifers (Barker, 1988), etc. target specific problems and cannot simulate the flow processes of this complex pumping test. A numerical layered cylindrical grid model is applied to improve the conceptual understanding of the system, especially the impact of quarries and to

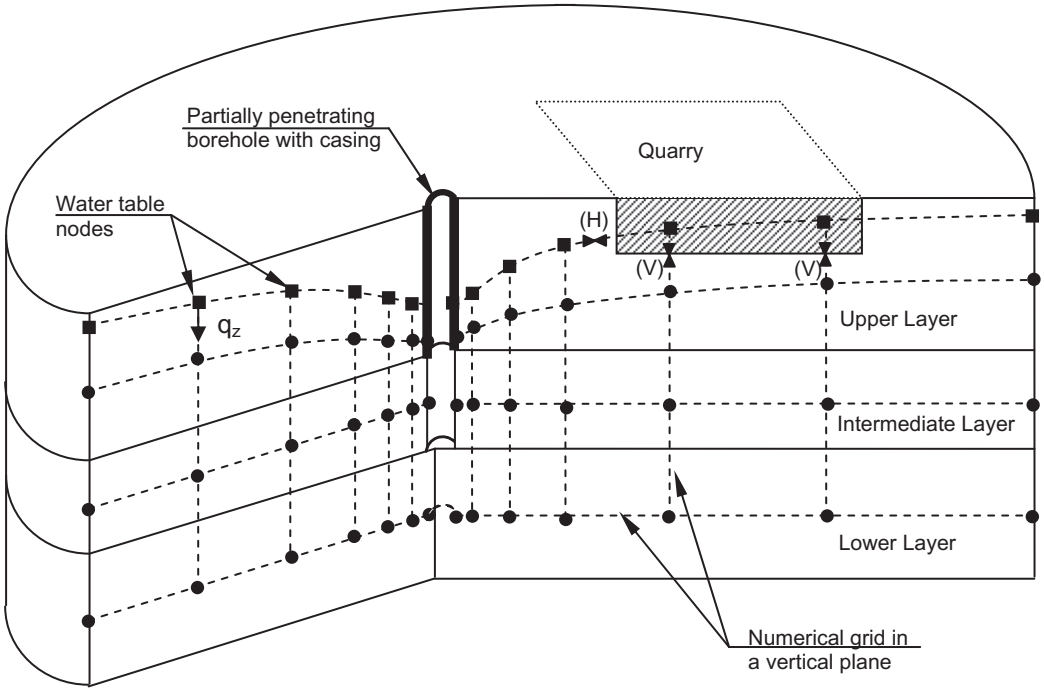

Fig. 3. Schematic representation of a multi-layered aquifer and the numerical representation of quarries.

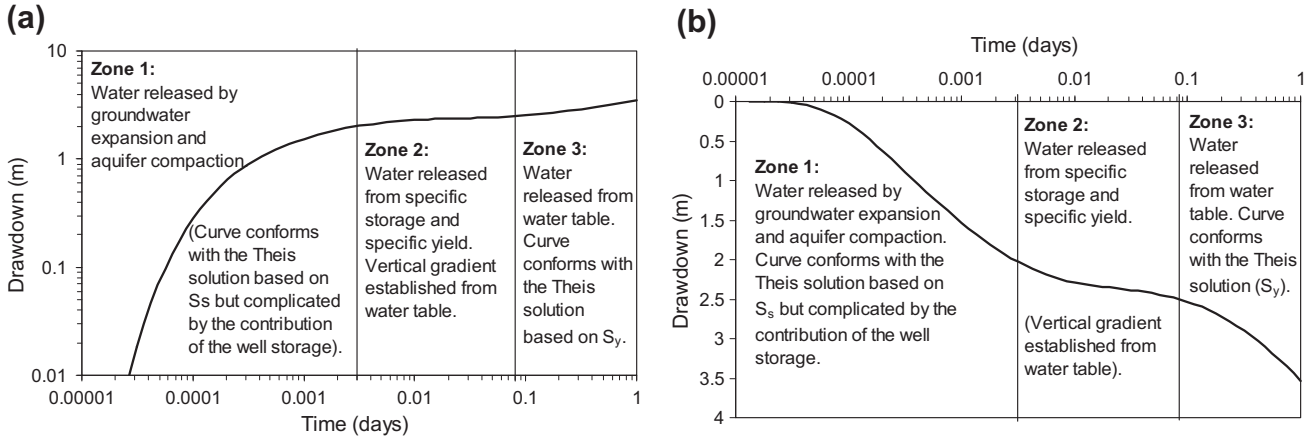

Fig. 4. A typical time-drawdown curve obtained from pumping in unconfined aquifers. (a) Log–log scale. (b) Log-arithmetic scale.

determine the values of the hydraulic parameters of the Chalk aquifer. This paper demonstrates that this numerical model is a flexible tool that can be applied to answer questions imposed by the conceptual model, in this case the effect of quarries, and improves it. It also demonstrates that despite the complexity of the Chalk groundwater system, the numerical model can reproduce satisfactorily much of the behaviour of the observed time-drawdown curves, allowing a better understanding of the aquifer hydraulic characteristics.

2. Materials and methods

The Swanscombe area is located on the south-eastern side of the London Basin (Fig. 1). It comprises the main valley of the River Thames, bordered by wide terraces, and Palaeogene age deposits over a Chalk plateau, which is terminated by an escarpment to the south. The Chalk has a maximum thickness of approximately 200 m and is partly covered by Palaeogene deposits comprising the Lambeth Group and the Thames Group. Along the Thames in the north of the area, the Chalk is overlain by terrace deposits and riverine alluvium. The regional hydraulic gradient slopes from the North Downs escarpment northwards towards the Thames. The area is drained by the River Thames to the north, the Rivers Cray and Darent in the west and the Rivers Ebbsfleet and Medway in the east. For further information about the regional hydraulic gradient refer to Darling et al. (2010).

Characteristic of the Swanscombe area is an abundance of raw materials that are utilised by the cement industry: chalk, clay and alluvial deposits are worked and gravel extraction is also common. Several sub-water-table quarries have been abandoned as the costs of dewatering have exceeded the rewards from quarrying. Other quarries are reaching their maximum development depth and, when they close, pumping will cease. Two quarries in

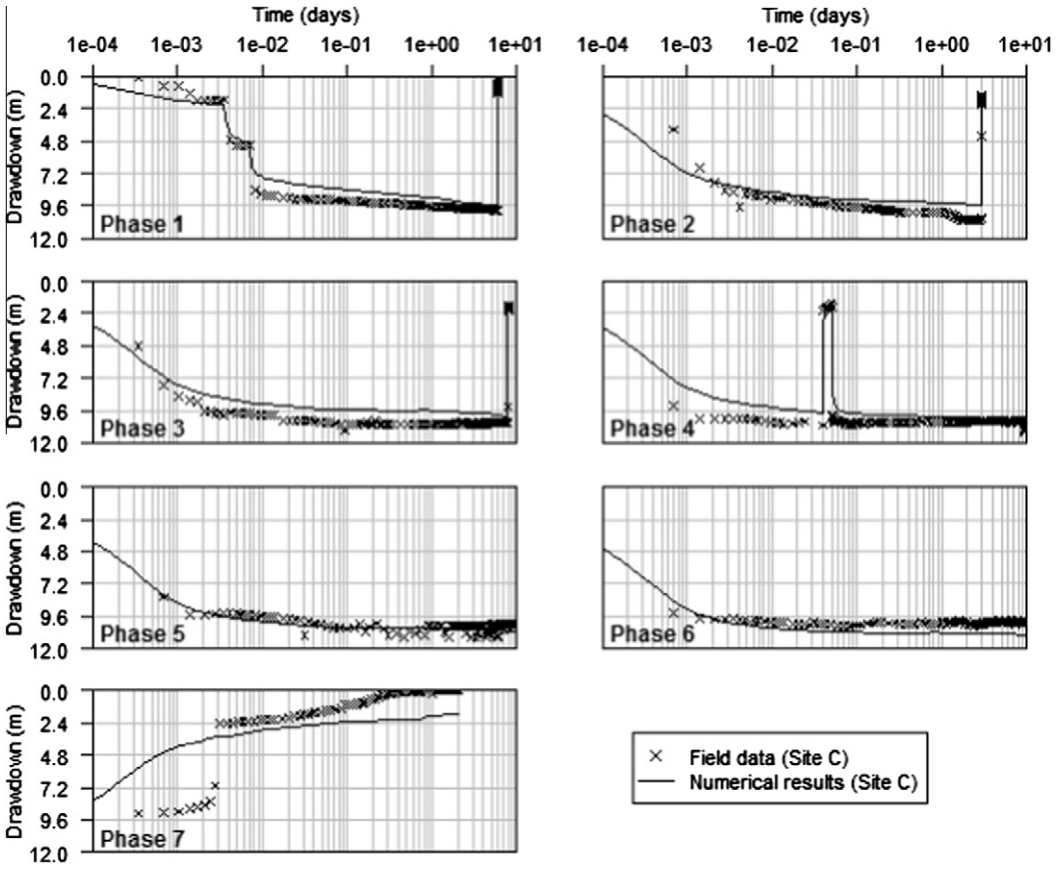

Fig. 5. Field and numerical time-drawdown curves at Site C abstraction borehole.

particular form the focus of this study; the Eastern Quarry, which is ceased operating in late 2007 and the Western Quarry, which has now been developed into a shopping centre.

The pumping test involved two abstraction wells plus four abstraction boreholes and 31 observation boreholes (Fig. 2). The two abstraction wells, defined as such on the basis of their large diameter size, are the Greenhithe abstraction well and the Southfleet abstraction well. Greenhithe abstraction well is located near the north-western corner of Eastern Quarry approximately 150 m from its western edge, and Southfleet abstraction well is close to the Eastern Quarry and located approximately 550 m from its eastern side (Fig. 2a). These two pumping wells are approximately 2700 m apart. The four abstraction boreholes, defined as such on the basis of their relatively small diameter size, are located in the area south of the quarries. These boreholes are: Site A (the Western Bean Farm borehole), Site B (the West Drudgeon Farm borehole), Site C (the Mid Drudgeon Farm borehole) and Site D (the West Beacon Wood borehole). Of the four abstraction boreholes, Site A is closest to the Greenhithe well at a distance of 1800 m and Site C is the closest to Southfleet at a distance of 2000 m. A distance of approximately 1300 m separates Sites A and C.

Pumping started on 18 October 2002 at sites A–C with abstraction rates of 19.0 l/s, 12.7 l/s and 77.5 l/s respectively. Abstraction at Site D started 8 days later at a rate of 49.0 l/s. Abstraction at Greenhithe and Southfleet started 28 days later at rates of 46.0 l/s and 37.0 l/s respectively. The abstraction at all sites ceased on the 16 December 2002 and the recovery at the abstraction boreholes was recorded for a further 2 days. During the pumping phase, abstraction was interrupted randomly at all the sites either because of generator failures or for generator maintenance, leading to unplanned recovery periods. This paper focuses on the results obtained at Site C and two of its neighbouring observation boreholes, boreholes 12 and 19, to illustrate the complexity of the Chalk groundwater system and the advantages of using the numerical radial flow model to simulate this groundwater system and analyse the pumping test results. The observed drawdown results are shown in Figs. 5 and 6.

3. Theory/calculation

The layered cylindrical grid numerical model uses the finite-difference method to solve the basic equation describing flow through a porous medium under confined and unconfined conditions. To simulate groundwater flow converging to a pumped well, the three-dimensional basic flow equation is written in cylindrical coordinates and the aquifer is discretised using a grid illustrated in Fig. 3. For confined aquifers and in terms of the drawdown (s) this equation is given by (Rushton, 2003):

$$K_r \frac{\partial^2 s}{\partial r^2} + \frac{K_r}{r}\frac{\partial s}{\partial r} + \frac{K_\theta}{r^2}\frac{\partial^2 s}{\partial \theta^2} + K_z \frac{\partial^2 s}{\partial z^2} = S_s \frac{\partial s}{\partial t} + N \quad (1)$$

where

- K_r, K_θ and K_z are the hydraulic conductivities in the radial, the circumferential and the vertical directions respectively (LT^{-1}).
- S_s is the specific storage (L^{-1}).
- N is an external source term (T^{-1}).
- r is the radius from the centre of the abstraction borehole to the point where the drawdown s is calculated (L).

In a layered system, the head values of Equation 1 are averaged over the layer saturated thickness and the horizontal hydraulic conductivity is replaced by the transmissivity of the layer. This does not apply at the uppermost layer if the groundwater system

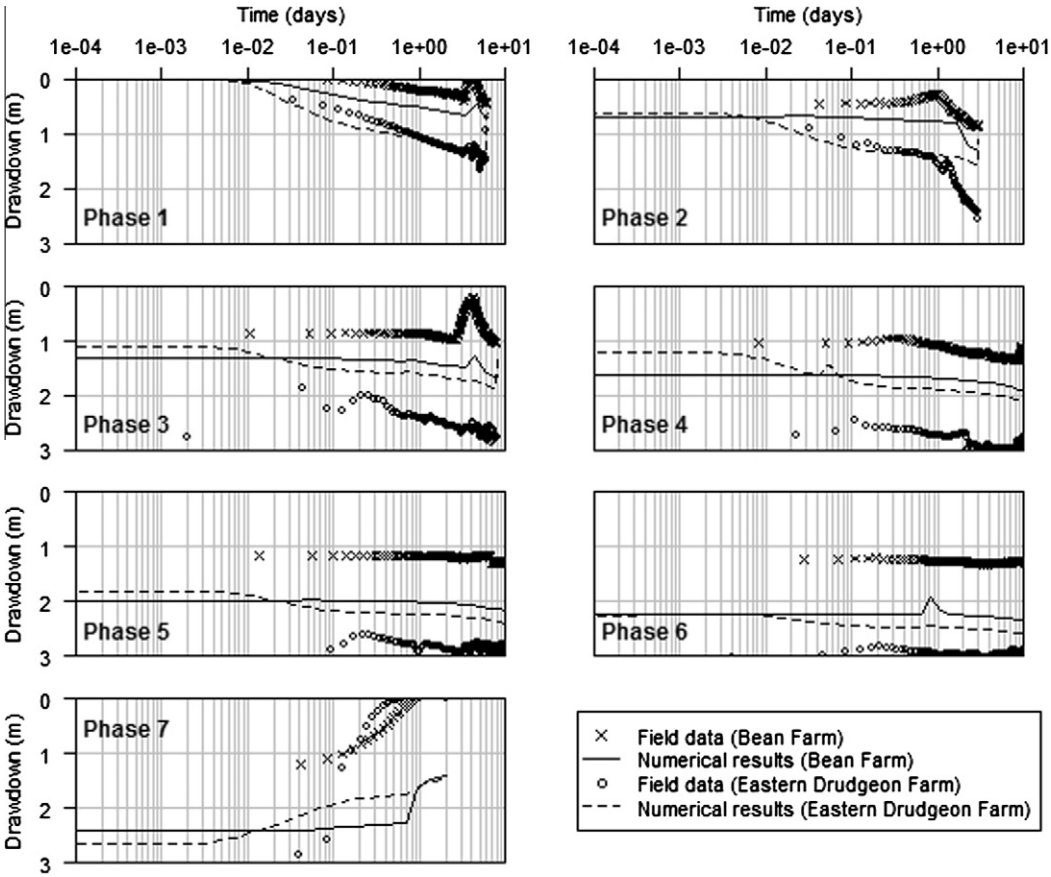

Fig. 6. Field and numerical time-drawdown curves at Bean Farm and Eastern Drudgeon Farm observation boreholes.

is under unconfined conditions. Under these conditions an additional numerical layer is created at the top of the uppermost layer of the model to represent the presence of the water-table (Fig. 3).

The equation that describes the movement of the water-table is discussed by Todsen (1971) and Neuman (1972) and is given by:

$$\frac{\partial \varphi}{\partial t} = \frac{-1}{n_e}\left(K_r \frac{\partial s}{\partial r}\frac{\partial \varphi}{\partial r} + \frac{K_\theta}{r^2}\frac{\partial s}{\partial \theta}\frac{\partial \varphi}{\partial \theta} - K_z \frac{\partial s}{\partial z}\right) \quad (2)$$

where:

- φ is a function that represents the location of the water-table and (L),
- n_e is the porosity of the aquifer (Dimensionless).

The complexity of this non-linear equation can be reduced by assuming that the product of the hydraulic gradients is small and can be neglected (Rushton and Redshaw, 1979). In this case Eq. (2) reduces to: $\frac{\partial \varphi}{\partial t} = \frac{1}{S_y}\left(K_z \frac{\partial s}{\partial z}\right)$ where the porosity is considered to be approximately equal to the specific yield S_y. By changing the subject, this equation can be written as: $K_z \frac{\partial s}{\partial z} = S_y \frac{\partial \varphi}{\partial t}$ and then by Darcy's law: $q_z = S_y \frac{\partial \varphi}{\partial t}$, allowing the term q_z to be added to the right hand side of Eq. (1), which is then applied only to the water-table nodes. The radial interval between nodes increases in a logarithmic pattern from the centre of the abstraction borehole where the numerical grid is centred to the outer boundary. This creates a large number of nodes close to the abstraction well and improves the representation of the steep hydraulic gradient as a result of pumping in the vicinity of the abstraction borehole. In contrast to a general saturated aquifer node, a water-table node changes its location vertically based on its head value calculated at the end of a time step (Fig. 3). This allows the aquifer to dewater as the water-table moves downwards and the saturated thickness of the uppermost layer becomes spatially variable. The vertical flow between nodes in different layers is determined by considering mass conservation at the interface between layers.

To represent the water contained within the abstraction well, i.e. well storage, the values storage coefficients of the nodes located inside the abstraction borehole and where pumping is applied are all set to unity. The occurrence of the seepage face is represented by acknowledging that the aquifer nodes located at the abstraction borehole face became subject to atmospheric pressure when the water levels inside the abstraction borehole drops below the base of their corresponding layers. When this happens the groundwater head values of these nodes are fixed to a value equal to the base elevations of their corresponding layers.

The model code has been developed in C++ programming language and benefits from the object-oriented technology. Information on the application of this technology in groundwater modelling can be found in the work of Spink et al. (2003) and Jackson et al. (2003). For a full description of the model and its application refer to Mansour (2003) and Mansour et al. (2003). This type of model is preferred to the Cartesian grid groundwater models that allow grid refinement such as ZOOMQ3D (Jackson et al., 2003) and MODFLOW 2005 (Harbaugh, 2005) because of its better representation of the flow processes taking place next to the abstraction borehole, e.g. well losses, well storage, seepage face, etc. In addition, although the Cartesian grid models yield accurate solutions at the observation boreholes, the solution at the abstraction borehole is less accurate. The inaccuracy at the abstraction borehole is primarily due to the structure of the Cartesian numerical grid, which does not allow the specification of nodes at the well face and consequently it is not possible to set the hydraulic conductance values between the node inside the well and its surrounding aquifer nodes correctly. In addition, it is not possible to set both the area and the perimeter of a rectangular cell

in a Cartesian model to be equal to the area and perimeter of the actual circular abstraction borehole at the same time. If the numerical grid is refined so that the area of the rectangular cell is equal to the area of the abstraction borehole the rectangular cell will have a perimeter that is smaller than the actual borehole perimeter. As the area through which groundwater is flowing from the aquifer to the abstraction borehole in the numerical model is smaller than in reality, it causes the simulated drawdown to be greater than the observed one.

The preprocessor, RADMOD (Reilley and Harbaugh, 1993), has been developed for MODFLOW (McDonald and Harbaugh, 1988) to simulate axi-symmetric flow to a well. The radial flow model reported here has the advantage of simulating the moving water-table, which cannot be done in RADMOD.

4. Results and discussion

4.1. Conceptual model

The Chalk aquifer is partly overlain by Palaeogene strata in the Swanscombe area (Figs. 1 and 2). However, the water-table is within the Chalk Formation almost everywhere and the Chalk is the only source of groundwater available for abstraction. While groundwater flow in the Chalk is complicated by the presence of fractures or high conductivity zones as demonstrated in the analysis of an earlier individual pumping test (Spink and Mansour, 2003), it has not been possible to determine the size, extents, and directions of these high conductivity zones. Consequently, these zones cannot be represented in details in the conceptual model and the Chalk aquifer is represented here using two uniform hydro-geological layers. The upper one, in which the high conductivity zones are better developed, is in direct contact with the abstraction borehole at Site C. The lower layer, which represents the remainder of the Chalk and is less well developed, is also included as it may contribute to the total water abstracted (Fig. 2b). Aquifer permeability values obtained from the analysis of the pumping test are related, therefore, to both the Chalk matrix and the fractures or high conductivity zones within it.

The layered cylindrical grid model can address conceptual complexities related to the representation of flow processes next to the abstraction borehole, the variation of pumping rates, and the simultaneous pumping from more than one borehole. However, the effects of the quarries on the pumping test results are not fully understood. The quarries may cause an increase in drawdown because of the reduced aquifer thickness in the zone where the aquifer is missing and through which groundwater flows are converging towards the abstraction well. Conversely, it may be also possible that the water held in the topographical depressions on the surface of these quarries provides the system with a source of water which compensates the effects of the missing part of the aquifer. These two conceptual representations of the quarries are investigated by the numerical model.

4.2. Overview of the test results: preliminary assessment

The time-drawdown curve of the first abstraction phase at Site C (Fig. 5 Phase 1) does not show the typical unconfined behaviour because of the step increases in the pumping rate at the start of the test. The typical behaviour of a time-drawdown curve in unconfined aquifers, as explained by Kruseman and de Ridder (1990), has an 'S' shape (Fig. 4a) when plotted on logarithmic axes. Each section of the *S* curve reflects the changes in the dominant process occurring in the aquifer. At early times, the abstracted water is released instantaneously from storage by the expansion of the water and the compaction of the aquifer. The unconfined aquifer effectively behaves as confined, but the time-drawdown curve may not match the Theis solution because of well storage, which delays the start of drawdown at the observation boreholes (Zone 1 of Fig. 4a). Once the water-table starts falling, the quantity of water released from specific yield (S_y) reduces the gradient of the intermediate-time segment and the time-drawdown curve is comparable to that obtained from a leaky aquifer (Zone 2 of Fig. 4a). In the third stage, the time-drawdown curve once again tends to conform to a Theis curve based on storage due to S_y. At this time, the water-table is the major contributor to the water abstracted from the aquifer (Zone 3 of Fig. 4a).

When plotted on logarithmic time and linear drawdown axes, the time-drawdown curve also takes a typical shape that can be divided into three segments. The first is a straight line that matches the Theis solution, if well storage is small (last part of the curve in Zone 1 of Fig. 4b). The second starts when the straight line changes gradient and flattens indicating that storage from water-table is contributing to the system. The length of the second segment depends on the vertical hydraulic conductivity and the specific yield of the aquifer (Zone 2 of Fig. 4b). The third segment starts when the rate of drawdown increases again reflecting the fall of the water-table (Zone 3 of Fig. 4b).

The plot of the first abstraction phase at Site C (Fig. 5 Phase 1) also shows a delayed increase in the drawdown values at the start of the test indicating the presence of a significant source of water which is likely to be well storage. The time-drawdown curves of the subsequent abstraction phases, however, show typical unconfined behaviour but do not reflect the expected water-table movement at later times. The presence of a larger well storage component is evident in these phases and is reflected by the delayed fall at the start of each phase. The field data collected during the recovery phase (Fig. 5 Phase 7) show a delayed initial rise that is probably due to problems in the measuring device and cannot be used to confirm this large well storage.

4.3. Numerical analysis

Site C abstraction borehole diameter is 0.42 m, with a depth of 137 m. It is cased to a depth of 75 m below the ground surface. A 43 m layer of Palaeogene deposits overlies the Chalk at this site but the initial water level is recorded at a depth of 77.1 m from the ground surface indicating that the water-table is not found within the Palaeogene strata. The pumping borehole is open along its full saturated depth. While the casing of the Site C abstraction borehole has a diameter of 0.42 m, geophysical well logging (Buckley, 2003) indicates that this borehole is larger than its nominal size in the open section. Accordingly, the well diameter used in the model is increased to 0.6 m, which is the average diameter shown by the borehole logs. The first part of the Chalk aquifer, which is in direct contact with the abstraction well, is approximately 60 m thick at this position (Fig. 2b). It is represented numerically by four layers, the three uppermost layers are 10 m thick and the lower one is 30 m thick. The narrow thicknesses of the first three layers allow the formation of the seepage face at the abstraction borehole wall. The second, deeper Chalk layer, which is not in contact with the abstraction borehole (Fig. 2b), is approximately 108 m thick and represented in the model by one numerical layer.

A three-dimensional model was built to improve the representation of the quarries and to improve the locations of the abstraction and observation boreholes within the model. In a single slice numerical model, i.e. assuming radial symmetry and simulating groundwater flow using the radial and vertical directions only, observation borehole 12 coincides with Site D abstraction borehole and observation borehole 17 coincides with Site B abstraction borehole. Consequently, it is not possible to simulate the groundwater

heads at the observation wells correctly as they coincide with the abstraction boreholes. The three-dimensional numerical model is built by replicating the vertical cross section described above fourteen times along different radial directions. The 14 slices provided a line of nodes along the radial direction next to the abstraction and observation boreholes of interest (Fig. 2a). In three-dimensional view the numerical model takes a form that is similar to the one shown in Fig. 3 but without the well casing. While the groundwater flow processes at borehole Site C are represented in detail, the remaining pumping boreholes are included in the model by assigning the corresponding abstraction to the nearest model node (Fig. 2a).

The model was calibrated by modifying the values of the aquifer hydraulic parameters until the simulated drawdown curves match the observed ones. Many trial values for the aquifer parameters were used to match the simulated and field time-drawdown curves. Commencing with parameter values suggested by previous studies of the Chalk (Allen et al., 1997), each trial involved changing the value of one parameter, based on the effects that this parameter has on the relevant time-drawdown curves. The parameters modified are: the horizontal and vertical hydraulic conductivities, the specific yield and the specific storage of each layer of the model. Possible values for the different hydraulic parameters can be established from this trial and error exercise. To improve the fit between the numerical and field results the parameter estimation package PEST (Doherty, 2004) was used. PEST is model-independent software that modifies the input files of the model and adjusts a preselected set of its parameters until the discrepancy between the field and numerical results are reduced to a minimum. PEST undertakes many model runs to optimise the parameter values and to perform uncertainty analysis. PEST was used here to refine the hydraulic parameter values and to estimate the uncertainty associated with these values.

Initially PEST was used without the inclusion of the quarries in the numerical model. The parameters modified by PEST were: the horizontal and vertical hydraulic conductivities, the specific yield and the specific storage, and the well loss factor. The values of the hydraulic parameters optimised by PEST, as well as the estimated 95% confidence limits, are given in Table 1. The optimised transmissivity value of the part of the Chalk that is in direct contact with the borehole is $1340\,m^2\,day^{-1}$. The optimised vertical hydraulic conductivity value is $0.86\,m\,day^{-1}$. The optimised storage coefficient and specific yield are $1\times10^{-5}\,m^{-1}$ and 0.012 respectively.

Subsequently, the quarries are added to the numerical model by altering the hydraulic connections between the nodes to either remove the volume represented by the quarries completely, or by reducing the thickness of the first layer of the Chalk, but assuming that the water stored within the quarry is significant and is available to be drawn by the abstraction boreholes. Two additional runs were undertaken to represent these conditions. In the first run the quarries were included in the model by introducing internal impermeable boundaries along the quarry walls in the uppermost numerical layer (numerical link (H) in Fig. 3). The nodes located within the quarry area, however, remained connected to the nodes underneath them by the mean of the vertical hydraulic conductivity (numerical links (V) in Fig. 3). Simulated drawdown values produced from this run did not show significant differences from the results when the quarry is ignored, because the internal boundaries do not greatly affect the results and the vertical hydraulic connection was enough to withdraw water from the specific yield storage of the nodes located within the quarry area. In the second run the vertical connections between the nodes located within the quarries and the nodes underneath them were both disconnected (Fig. 3). This run assumed that the quarried Chalk was absent. The simulated drawdown values were influenced by the disconnection of the nodes within the quarries, especially at the end of the abstraction phases. These are the results presented in Figs. 5 and 6.

Table 1
Optimised hydraulic parameter values and the 95% confidence limits.

Parameter	Estimated value	95% confidence limits	
		Lower limit	Upper limit
Horizontal hydraulic conductivity K_h ($m\,day^{-1}$)	22.33	20.5	24
Vertical hydraulic conductivity K_v ($m\,day^{-1}$)	0.086	0.065	0.107
Specific storage S_s (m^{-1})	1e−05	5.5e−06	14.5e−5
Specific yield S_y (dimensionless)	0.012	0.0087	0.015
Well loss factor (dimensionless)	0.09	0.072	0.109

Fig. 5 shows a comparison between the simulated and observed drawdown values at the abstraction borehole C. The numerical model reproduced satisfactorily the steps in the time-drawdown curve of the first abstraction phase. In addition, the simulated drawdown values and the gradient of the time-drawdown curve from 0.01 days follow the observed ones, indicating that the hydraulic parameters used in the numerical model are representative to the overall hydraulic characteristics of the aquifer. The slight drawdown observed at approximately 1 day was produced after the inclusion of quarries in the numerical model. The delayed decline recorded in the field data (Fig. 5 Phase 2) suggests the presence of a larger well storage component than is evident in the other phases. The field data collected during the recovery phase (Fig. 5 Phase 7) show a delayed initial rise, but this may be due to a problem with the measuring device. However, the numerical results do show an acceptable level of recovery compared to the field data when abstraction is interrupted in the fourth abstraction phase (Fig. 5 Phase 4).

Many of the observation boreholes show little response to pumping at the abstraction boreholes and some of the observation boreholes show fluctuations in groundwater levels that cannot be related to the pumping test. The only time-drawdown curves that show reasonable correlation to abstraction at Site C are those at Bean Farm borehole and Eastern Drudgeon Farm borehole, which are situated approximately 920 m and 240 m away from abstraction borehole C (Boreholes 12 and 19 in Fig. 2a). The match between the simulated and drawdown values of the first two abstraction phases is acceptable, indicating that the hydraulic conductivity and the storage coefficient values, which control the gradient of the time-drawdown curve and the start of drawdown respectively, are representative of the hydraulic characteristics of the aquifer (Fig. 6). The behaviour of the simulated time-drawdown curves over the remaining abstraction phases is comparable to the observed ones, but there are vertical shifts between them. This is caused by the sudden drop in drawdown values at the end of the second abstraction phase and is particularly evident in the Eastern Drudgeon Farm borehole. This behaviour can be caused by the presence of fractures that dry up when the water-table falls beneath them leading to significant change in the transmissivity of the Chalk aquifer. Fractured or high conductivity zones can be modelled using the layered cylindrical grid model. However, in this instance it was decided to concentrate on the impact of the quarries on the groundwater system.

5. Conclusion

This paper discusses the analysis of a complex pumping test undertaken in the Chalk aquifer of the Swanscombe area, south-east London, using a numerical layered cylindrical grid model. The complexity of the Swanscombe pumping test arises

from factors such as abstraction from a partially penetrating abstraction borehole, the stepwise increase of abstraction, the unplanned intermittent stoppages of pumping during the test period and simultaneous pumping from adjacent boreholes. In addition, the test results were affected by the presence of major quarries in the area. Two scenarios are used to study the impact of the quarries on the test results. In the first scenario, a quarry is represented in the model by imposing internal impermeable boundaries along the locations of its walls whilst allowing the water stored within it to contribute to the groundwater system. Quarries in this scenario did not impact the simulated results. In the second scenario, in addition to the internal no flow boundaries, the volume of water held by the quarries are completely removed from the model. This quarry representation caused additional drawdown at the end of the abstraction phases and improved the match between the observed and simulated time-drawdown curves. This numerical configuration is used to estimate the hydraulic parameter values of the aquifer.

The numerical results showed that a transmissivity value of 1340 m^2 day^{-1} of the part of the Chalk that is in direct contact with the borehole, a vertical hydraulic conductivity value of 0.86 m day^{-1}, and a storage coefficient and a specific yield of 1×10^{-5} m^{-1} and 0.012 respectively produce a good match between the observed and simulated time-drawdown curves. The use of the numerical model permitted the deployment of the parameter estimation software PEST (Doherty, 2004) to optimise the values of the hydraulic parameters and to undertake uncertainty analysis. It was found that the highest uncertainty was associated with the value of the storage coefficient with the 95% confidence limits being approximately 45% greater or smaller than the estimated value. The second highest uncertainty is associated with the values of the specific yield and vertical hydraulic conductivity with the 95% confidence limits being approximately 25% greater or smaller than the estimated values (Table 1). These values fall within the limits reported in the literature for Chalk aquifers (see for example Allen et al., 1997) and can be used to specify the hydraulic parameter values for this site in a regional Cartesian model.

This paper demonstrates that the layered cylindrical grid model used in this study can incorporate enough mechanisms to reproduce the complex behaviour of the time-drawdown curve and has many advantages on the use of conventional analytical solutions and on the Cartesian models which are not designed to simulate groundwater flow converging to a pumped borehole. This work also demonstrates that the cylindrical grid numerical model is a powerful tool for analysing the pumping test results. It provides useful information on both the well performance and the hydraulic characteristics of the aquifer. This helps improving the conceptual model of aquifers such as the complex Chalk aquifer.

Acknowledgments

The authors thank the anonymous reviewers and BGS internal reviewers Mrs Ann Williams and Dr Vanessa Banks for improving the manuscript. The paper is published by permission of the Director, British Geological Survey (Natural Environment Research Council).

References

Allen, D.J., Brewerton, L.J., Colbey, L.M., Gibbs, B.R., Lewis, M.A., Macdonald, A.M., Wagstaff, S.J., Williams, A.T., 1997. The physical properties of major aquifers in England and Wales. British Geological Survey Technical Report WD/97/34. Environment Agency R & D Publication 8.

Barker, J., 1988. A generalised radial-flow model for pumping tests in fractured rock. Water Resources Research 24 (10), 1796–1804.

Boulton, N.S., 1954. The drawdown of a water-table under non-steady conditions near a pumped well in an unconfined formation. In: Proceedings of the Institution of Civil Engineers, vol. 3, Part 3, pp. 564–579.

BSI, 1992. Code of practice for Test pumping of water wells. BS 6316: 1992. London, UK.

Buckley, D., 2003 Swanscombe Phase 2a Task 2.2 Geophysical Logging. British Geological Survey Technical Report. CR/01/239C.

Cooper, H.H., Jacob, C.E., 1946. A generalized graphic method for evaluating formation constants and summarizing well-field history. Transactions of American Geophysical Union 27 (4), 526–534.

Dagan, G., 1967. Linearised solutions of free surface groundwater flow with uniform recharge. Journal of Geophysical Research 72 (4), 1183–1193.

Darling, W.G., Gooddy, D.C., Riches, J., Wallis, I., 2010. Using environmental tracers to assess the extent of river–groundwater interaction in a quarried area of the English Chalk. Applied Geochemistry 25, 923–932.

Doherty, J., 2004. PEST: model-independent parameter estimation user manual. Watermark Numerical Computing.

Gambolati, G., 1976. Transient free surface flow to a well: an analysis of theoretical solutions. Water Resources Research 12 (1), 27–39.

Hantush, M.S., Jacob, C.E., 1955. Non-steady radial flow in an infinite leaky aquifer. Transactions of the American Geophysical Union 36, 95–100.

Harbaugh, A.W., 2005. MODFLOW 2005, The US Geological Survey modular groundwater model-the Ground-Water Flow Process: US Geological Survey Techniques and methods 6-16, variously p.

Kruseman, G.P., de Ridder, N.A., 1990. Analysis and evaluation of pumping test data. The International Institute for Land Reclamation and Improvement. Publication 47.

Jackson, C.R., Hughes, A.G., Mansour, M.M., Spink, A.E.F., Bloomfield, J.P., Riches, J., Jones, M.A., 2003. Numerical modelling of a multiple-well pumping test using a locally refined, object-oriented regional groundwater model. In: MODFLOW and More 2003: Understanding through modelling, Conference Proceedings, Golden, CO, September 2003, pp. 383–387.

Mansour, M.M., 2003. Flow to wells in unconfined aquifers using mesh refinement and object-oriented technology. Ph.D. thesis. The University of Birmingham, UK.

Mansour, M.M., Spink, A.E.F., Riches, J., 2003. Numerical investigation of flow to pumped wells in heterogeneous layered aquifers using radial flow models. In: MODFLOW and More 2003: Understanding through modelling, Conference Proceedings, Golden, CO, September 2003, pp. 388–392.

McDonald, M.G., Harbaugh, A.W., 1988. A Modular Three-dimensional Finite-difference Ground-water Flow Model. Technical Report, US Geol. Survey, Reston, VA.

Moench, A.F., 1993. Computation of type curves for flow to partially penetrating wells in water-table aquifers. Ground Water 31, 966–971.

Moench, A.F., 1994. Specific yield as determined by type-curve analysis of aquifer-test data. Ground Water 6 (2), 37–46.

Moench, A.F., 1997. Flow to a well of finite diameter in a homogeneous, anisotropic water table aquifer. Water Resources Research 33 (6), 1397–1407.

Neuman, S.P., Witherspoon, P.A., 1971. Analysis of non-steady flow with a free surface using the finite element method. Water Resources Research 7 (3), 611–623.

Neuman, S.P., 1972. Theory of flow in unconfined aquifers considering delayed response of the water table. Water Resources Research 8 (4), 1031–1045.

Neuman, S.P., 1974. Effect of partial penetration on flow in unconfined aquifers considering delayed gravity response. Water Resources Research 10 (2), 303–312.

Neuman, S.P., 1979. Perspective on delayed yield. Water Resources Research 15, 899–908.

Reilley, T.E., Harbaugh, A.W., 1993. Simulation of cylindrical flow to a well using the US Geological Survey modular finite-difference groundwater flow model. Ground Water 31 (3), 489–494.

Rushton, K.R., 2003. Groundwater Hydrology. Conceptual and Computational Model. John Wiley and Sons Ltd., Chichester, UK.

Rushton, K.R., Redshaw, S.C., 1979. Seepage and Groundwater Flow. John Wiley and Sons, Chichester, UK.

Streltsova, T.D., 1972. Unsteady radial flow in an unconfined aquifer. Water Resources Research 8 (4), 1059–1066.

Streltsova, T.D., 1973. Flow near a pumped well in an unconfined aquifer under nonsteady conditions. Water Resources Research 9 (1), 227–235.

Spink, A.E.F., Jackson, C.R., Hughes, A.G., Hulme, P.J., 2003. The benefits of object-oriented modelling demonstrated through the development of a regional groundwater model. In: MODFLOW and More 2003: Understanding Through Modelling, Conference Proceedings, Golden, CO, September 2003, pp. 336–340.

Spink, A.E.F., Mansour, M.M. 2003. Swanscombe Phase 2. Task 6: Preliminary Modelling. Report prepared for the British Geological Survey. Wallingford, England.

Theis, C.V., 1935. The relation between the lowering of the piezometric surface and the rate and duration of discharge of a well using groundwater storage. Transactions of the American Geophysical Union, 16th Annual Meeting, pp. 519–524.

Todsen, M., 1971. On the solution of transient free-surface problems in porous media by finite-difference methods. Journal of Hydrology 12, 177–210.